Attractive Set of Optimal Feedback Control for the Hill Three-Body Problem

Bando, Mai
Department of Aeronautics and Astronautics, Kyushu University : Associate Professor

Scheeres, Daniel J.
Aerospace Engineering Sciences, University of Colorado at Boulder : A. Richard Seebass Endowed Chair Professor

出版情報：Journal of Guidance, Control, and Dynamics. 39 (12), pp.2725-2739, 2016-12. American Institute of Aeronautics and Astronautics
バージョン：
権利関係：

Attractive Set of Optimal Feedback Control for the Hill Three-Body Problem

Mai Bando*

Kyushu University, 744 Motooka, Nishu-ku, Fukuoka 819-0395, Japan

Daniel J. Scheeres†

University of Colorado at Boulder, Boulder, Colorado 80309

ABSTRACT

This paper investigates the combination of optimal feedback control with the dynamical structure of the three-body problem. The results provide new insights for the design of continuous low-thrust spacecraft trajectories. Specifically we solve for the attracting set of an equilibrium point or a periodic orbit (represented as a fixed point) under optimal control with quadratic cost. The analysis reveals the relation between the attractive set and original dynamics. In particular we find that the largest dimensions of the set are found along the stable manifold and the least extent is along the left eigenvector of the unstable manifold. The problem is worked out in detail analytically and we develop several proofs regarding the structure of the attractive set for an optimal transfer. Our result is theoretical and developed for a linearized system, but can be extended to nonlinear and more realistic situations.

1 Introduction

The stable and unstable manifold associated with a family of periodic orbits has been exploited for the trajectory design in the three-body problem [1–4]. In simple terms, in order to realize transfer without fuel expenditure, the spacecraft should be placed onto the stable manifold associated with the desired orbit. Once the spacecraft is placed on the manifold, the natural dynamics steer the spacecraft into its final orbit. The Genesis trajectory is known as an example of this kind of transfer [4]. The recent ARTEMIS mission involved significant operations about the EarthMoon L_1 and L_2 points using dynamical structure of libration point dynamics [5].

Recently, low-thrust propulsion has been studied together with multi-body systems. Due to the very small accelerations often considered, the resulting trajectory designs often span long time periods. Due to

*Associate Professor, Department of Aeronautics and Astronautics, mbando@aero.kyushu-u.ac.jp, Member AIAA.

†A. Richard Seebass Endowed Chair Professor, Aerospace Engineering Sciences, Fellow AIAA.

this the use of continuous low-thrust in trajectory design can significantly increase the complexity of the design process. Moreover, analytical theory is not generally available for the multi-body problem, while it is well developed for the two-body problem. Despite these complications, low-thrust trajectory design in multi-body systems has been extensively applied to transfers to the Moon [6–8], to Mars [9–11], to Venus [12], to Near Earth Objects [13] and to the libration point orbits in the Sun-Earth and Earth-Moon systems in [14, 15], although generally relying solely on numerical approach.

The application of optimal control for trajectory design has been extensively studied in the literature [16]. For Keplerian dynamics, the optimal transfer problem related to the property called null controllable with vanishing energy (NCVE) is studied in [17]. This is a property that any state of the system can be steered to the origin with an arbitrarily small amount of control energy in the L_2 (square integral) sense. From a dynamical systems point of view, any state on the stable or center manifold can be controlled with an arbitrarily small amount of control energy. For the three-body system, dynamical structures related to optimal control have been studied in [18]. Attainable sets to incorporate low-thrust trajectory into the invariant manifolds technique is proposed in [19].

This paper investigates the combination of optimal feedback control with the dynamical structure of the three-body problem, using a quadratic acceleration cost. The set of all initial states which can reach the desired state with a given optimal control cost forms an ellipsoid called the attractive set. We prove that the attracting set of a general unstable equilibrium point or periodic orbit has a canonical structure that can be described using the system dynamics, specifically using the unstable eigenvalue and eigenvectors. These general results should hold for all astrodynamic systems and provide a systematic approach for optimal rendezvous with an equilibrium point or periodic orbit using low-thrust.

For this study, we exclusively focus on a linearized system around the libration point and libration point orbits, the former described by a linear time-invariant system and the latter by a time-periodic linear system. The controllability grammian plays an important role in this context. In control theory, the representation of input as quadratic forms involving the grammians is a classical result which arises in connection with the solution of finding the control input which expends the least energy [20]. We start with an attractive set of an equilibrium point in the linearized dynamics of the Hill's approximation of the three-body problem and then consider the attractive set of a periodic orbit. In particular we find that the largest dimensions of the set are found along the stable manifold and the least extent is along the left eigenvector of the unstable manifold. The problem is worked out in detail analytically and we develop several proofs regarding the structure of the attractive set for an optimal transfer to an equilibrium point and a fixed point. Specifically, we employ the positive definite solution of the differential Lyapunov equation and the difference Lyapunov equation to solve the attractive set for the finite time interval.

The paper is structured as follows. We first review necessary items from optimal control theory in Sec. 2. Section 3 provides the main theoretical results. In Sec. 4, examples are given to demonstrate the main results for a 1-DOF system, an equilibrium point in the Hill 3-Body problem, a Lyapunov orbit in the Hill 3-Body problem and a halo orbit in the Hill 3-Body problem. Section 5 gives closing remarks.

2 General theory of optimal control

In this Section, the minimum fuel problem with fixed terminal state for a general linear time-varying system is reviewed. By using the state transition matrix of the Hamiltonian system of the state and adjoint equations, the optimal cost is explicitly expressed in a closed manner. Then the attractive set is introduced as the contour of the optimal cost.

Optimal control problem for fixed terminal state

Consider the minimum fuel problem for a general linear time-varying system

$$\dot{x} = A(t)x + B(t)u, \tag{1}$$

$$J = \frac{1}{2}\int_{t_0}^{t_f} \|u\|^2 dt \tag{2}$$

where $x \in \mathbb{R}^n$ is a state, $u \in \mathbb{R}^m$ is control, $A(t) \in \mathbb{R}^n \times \mathbb{R}^n$ and $B(t) \in \mathbb{R}^n \times \mathbb{R}^m$. We assume that the system is controllable and the control is unconstrained. The boundary conditions are given as

$$x(t_0) = x_0, \;\; x(t_f) = 0 \tag{3}$$

Along the optimal trajectory, the state and adjoint follow the canonical equation and can be written as a Hamiltonian system

$$\begin{bmatrix} \dot{x} \\ \dot{p} \end{bmatrix} = \begin{bmatrix} A(t) & -B(t)B(t)^T \\ 0 & -A(t)^T \end{bmatrix} \begin{bmatrix} x \\ p \end{bmatrix} \triangleq A_H \begin{bmatrix} x \\ p \end{bmatrix} \tag{4}$$

where $p \in \mathbb{R}^n$ is the adjoint vector. Introduce the state transition matrix that solves Eq. (4) as

$$\Phi(t, t_0) = \begin{bmatrix} \phi_{xx}(t, t_0) & \phi_{xp}(t, t_0) \\ \phi_{px}(t, t_0) & \phi_{pp}(t, t_0) \end{bmatrix} \tag{5}$$

Then the optimal control is given by [21, 22]

$$u^*(t) = -B^T \phi_{pp}(t, t_0)\phi_{xp}^{-1}(t_f, t_0)\phi_{xx}(t_f, t_0)x_0 \tag{6}$$

Optimal cost function and attractive set of optimal control

The optimal cost function J^* is given by

$$J^* = \frac{1}{2}\int_{t_0}^{t_f} u^{*T}(t)u^*(t)dt = \frac{1}{2}x_0^T W_c^{-1}(t_f, t_0)x_0 \tag{7}$$

where

$$W_c^{-1}(t_f, t_0) = \left(\int_{t_0}^{t_f} \phi_{pp}^T(\tau, t_0)BB^T\phi_{pp}(\tau, t_0)d\tau\right)^{-1} \tag{8}$$

From the controllability of the system, $W_c(t, t_0)$ is positive-definite for $t > 0$, W_c^{-1} can also be defined for $W_c > 0$. Equation (7) forms an n-dimensional ellipsoid. If an initial state x_0 lies inside the ellipsoid

$$\mathscr{E}(c) = \{x_0 \in R^n | \frac{1}{2} x_0^T W_c^{-1}(t_f, t_0) x_0 \leq c\} \tag{9}$$

then the cost of the trajectory is less than c. Therefore the ellipsoidal set $\mathscr{E}(c)$ represents the attractive region associated with the optimal control (6) of cost $J^* \leq c$. The shape of the ellipsoid can be described by the eigenvalues and eigenvectors of the controllability grammian W_c. From the relation [20]

$$\lambda_{min}(W_c^{-1}(t_f, t_0))\|x_0\|^2 \leq x_0^T W_c^{-1}(t_f, t_0) x_0 \leq \lambda_{max}(W_c^{-1}(t_f, t_0))\|x_0\|^2 \tag{10}$$

the largest distance of attractive set is defined by $\lambda_{max}(W_c^{-1}(t_f, t_0))$ and the smallest one is is defined by $\lambda_{min}(W_c^{-1}(t_f, t_0))$.

Controllability Grammian

$W_c(t, 0)$ in Eq.(8) is called the controllability grammian which is defined as

$$W_c(t, t_0) = \int_{t_0}^{t} \phi(t_0, \tau) B B^T \phi^T(t_0, \tau) d\tau \tag{11}$$

for some $0 < t < \infty$. The system is controllable in an interval $[t_0, t]$ if the controllability grammian $W_c(t_0, t)$ is nonsingular. For the linear time-invariant system, it is reduced to

$$W_c(t, t_0) = \int_{t_0}^{t} e^{A(t_0-\tau)} B B^T e^{A^T(t_0-\tau)} d\tau \tag{12}$$

and the pair (A, B) is controllable if and only if the matrix $W_c(t_0, t)$ is nonsingular, for any $t > t_0$. The controllability grammian can be obtained as the solution to the differential Lyapunov equation:

$$\dot{W}_c(t) = A(t) W_c(t) + W_c(t) A^T(t) + B B^T, \;\; W_c(t_0) = 0 \tag{13}$$

For the stable and controllable time invariant system, $W_c(\infty) = \lim_{t\to\infty} W_c(t, t_0)$ exists and satisfies the Lyapuonv equation:

$$0 = A W_c(\infty) + W_c(\infty) A^T + B B^T \tag{14}$$

As shown in Appendix B, the optimal cost function J^* for a fixed point case is characterized by the controllability grammian for a discrete system which is defined as:

$$Y(k) = \sum_{j=0}^{k-1} e^{-MTj} \left(\int_0^T \phi_{pp}^T(\tau, 0) B B^T \phi_{pp}(\tau, 0) d\tau \right) e^{-M^T T j} \tag{15}$$

The discrete system $x(k+1) = Ax(k) + Bu(k)$ is controllable if and only if the matrix $Y(k)$ is nonsingular for any $k > 0$. The controllability grammian can be obtained as the solution to the difference Lyapunov equation:

$$Y(k+1) = A Y(k) A^T + B B^T, \;\; Y(0) = 0 \tag{16}$$

Suppose $x(k+1) = Ax(k) + Bu(k)$ is stable and controllable, then $Y(\infty) = \lim_{k\to\infty} Y(k)$ exists and satisfies the Lyapuonv equation:

$$Y(\infty) = A Y(\infty) A^T + B B^T \tag{17}$$

3 Main results

Theorem 3.1. *The asymptotic form of the attractive set to an equilibrium point or a fixed point under optimal control is completely defined by its left unstable eigenvectors and a term proportional to its unstable eigenvalue.*

We first consider the case of the attractive set to an equilibrium point. The following Lemmas allows us to describe the attracting set of optimal control in terms of eigenstructure of the original dynamics.

Attractive set of a linear time-invariant system

Consider the optimal control problem for a general linear time-invariant system

$$\dot{x} = Ax + Bu, \;\; x(0) = x_0, \; x(t_f) = 0 \tag{18}$$

Define the linear transformation

$$\boldsymbol{x} = T\boldsymbol{z}, \;\; \boldsymbol{z}^T = \begin{bmatrix} \boldsymbol{z}_s & \boldsymbol{z}_u & \boldsymbol{z}_c \end{bmatrix}$$

where T is the invertible matrix. Then Eq. (18) becomes

$$\dot{z} = \bar{A}\boldsymbol{z} + \bar{B}u, \quad \boldsymbol{z}(0) = T^{-1}\boldsymbol{x}_0 \tag{19}$$

where

$$\bar{A} = T^{-1}AT = \begin{bmatrix} A_s & & 0 \\ & A_u & \\ 0 & & A_c \end{bmatrix}, \quad \bar{B} = T^{-1} = \begin{bmatrix} B_s \\ B_u \\ B_c \end{bmatrix} \tag{20}$$

where A_s, A_u and A_c have eigenvalues with negative, positive and zero real parts respectively.

Let $\boldsymbol{u}_i$ and $\boldsymbol{v}_i$ $(i = 1, \cdots n)$ be right and left (generalized) eigenvectors corresponding to eigenvalue λ_i respectively. Then

$$T = \begin{bmatrix} \boldsymbol{u}_1 & \cdots & \boldsymbol{u}_n \end{bmatrix} \triangleq \begin{bmatrix} U_s & U_u & U_c \end{bmatrix}, \tag{21}$$

$$T^{-1} = \begin{bmatrix} \boldsymbol{v}_1^T \\ \vdots \\ \boldsymbol{v}_n^T \end{bmatrix} \triangleq \begin{bmatrix} V_s^T \\ V_u^T \\ V_c^T \end{bmatrix} \tag{22}$$

Note that the left and right eigenvectors are related to each other as

$$\boldsymbol{v}_i^T \boldsymbol{u}_j = \begin{cases} 1 & i = j \\ 0 & i \neq j \end{cases}$$

Then the following Lemma holds.

Lemma 3.1. *For a linear time-invariant system* (18)*,* W_c^{-1} *as* t_f *goes to infinity becomes*

$$W_c^{-1}(\infty) = T^{-T} \begin{bmatrix} 0 & 0 & 0 \\ 0 & W_{uu}^{-1} & 0 \\ 0 & 0 & 0 \end{bmatrix} T^{-1} \tag{23}$$

where W_{uu} *is solution to the Lyapunov equation:*

$$(-A_u)W_{uu} + W_{uu}(-A_u^T) + B_u B_u^T = 0 \tag{24}$$

Moreover, the eigenstructure of W_c^{-1} *is described as*

$$W_c^{-1}(\infty) = V_u W_{uu}^{-1} V_u^T \tag{25}$$

Proof. See Appendix A. □

Attractive set of a linear time-periodic system

Next, we consider the attractive set of a give periodic orbit Γ. The linearization about Γ is defined as the linear time-periodic system:

$$\dot{x} = A(t)x + Bu, \;\; x(0) = x_0 \tag{26}$$

where $A(t)$ is T-periodic function of time t for all $t \in \mathbb{R}$. From Floquet's theorem [23], the state transition matrix for one period $\phi_{xx}(T, 0)$ can be written in the form

$$\phi_{xx}(T, 0) = e^{MT}$$

where M is a constant matrix. From the symplecticity, $\phi_{pp}(T, 0)$ is given by

$$\phi_{pp}(T, 0) = e^{-M^T T}$$

Let T be the transformation matrix such that $T^{-1}MT$ is a block diagonal form. Then we can define

$$\bar{A} = T^{-1}e^{MT}T = \begin{bmatrix} A_s & & 0 \\ & A_u & \\ 0 & & A_c \end{bmatrix}, \quad \bar{B} = T^{-1} = \begin{bmatrix} B_s \\ B_u \\ B_c \end{bmatrix} \tag{27}$$

where A_s, A_u, and A_c has the characteristic exponents of $\Gamma(t)$ with negative, positive and zero real parts. Let $\boldsymbol{u}_i$ and $\boldsymbol{v}_i$ $(i = 1, \cdots n)$ be right and left eigenvector of eigenvalue λ_i respectively. The right and left eigenvectors corresponding to the eigenvalues of M can be defined as in the time-invariant case.

Lemma 3.2. *For a linear time-periodic system* (26)*,* W_c^{-1} *as* t_f *goes to infinity becomes*

$$W_c^{-1}(\infty) = \lim_{k \to \infty} Y^{-1}(k) = T^{-T} \begin{bmatrix} 0 & 0 & 0 \\ 0 & Y_{uu}^{-1} & 0 \\ 0 & 0 & 0 \end{bmatrix} T^{-1} \tag{28}$$

where Y_u is solution to the Lyapunov equation:

$$A_u^{-1} Y_{uu} A_u^{-T} + \left(\int_0^T \phi_{uu}^T(\tau, t_0) B_u B_u^T \phi_{uu}(\tau, t_0) d\tau \right) = 0 \tag{29}$$

where A_u is the unstable part of e^{MT} and ϕ_{uu} is state transition matrix of the unstable subsystem. Moreover, the eigenstructure of $W_c^{-1}(\infty)$ is described as

$$W_c^{-1}(\infty) = V_u Y_{uu}^{-1} V_u^T \tag{30}$$

Proof. See Appendix B. □

The fundamental difference between Lemma 3.1 and Lemma 3.2 is that system is discrete-time in Lemma 3.2 rather than continuous time as in Lemma 3.1. The proof of Theorem 3.1 follows immediately from Lemmas 3.1 and 3.2.

4 Applications

To illustrate the theory, a simple 1-DOF system is considered. Then specific examples of the attractive set of optimal control about an equilibrium point and libration point orbits of Hill's three-body problem are studied.

4.1 Attractive set for 1-DOF system

To illustrate the behavior of the attractive set for stable and unstable systems, let us start from a 1-DOF dynamical system

$$\ddot{r} + \alpha r = u \tag{31}$$

where u is the scalar control input. This system can be described by three different types of motion depending on the parameter α: if $\alpha > 0$ motion is is oscillatory, if $\alpha = 0$, it is rectilinear (degenerate), and if $\alpha < 0$, it is hyperbolic [24]. The state space form of (31) is given by

$$\dot{x} = Ax + Bu, \quad x = \begin{bmatrix} r(t) \\ \dot{r}(t) \end{bmatrix}, \quad A = \begin{bmatrix} 0 & 1 \\ -\alpha & 0 \end{bmatrix}, \; B = \begin{bmatrix} 0 \\ 1 \end{bmatrix} \tag{32}$$

It can be easily confirmed that the pair (A,B) is controllable. Consider the minimum fuel performance index:

$$J = \frac{1}{2} \int_{t_0}^{t_f} u^2 dt$$

In the following, the explicit form of the attractive set of the optimal control (9) is found for each case.

(i) Oscillatory Motion: $\alpha = \omega^2 > 0$

The state transition matrix is explicitly given by

$$\phi_{xx}(t) = e^{At} = \begin{bmatrix} \cos(\omega t) & \frac{1}{\omega}\sin(\omega t) \\ -\omega \sin(\omega t) & \cos(\omega t) \end{bmatrix} \tag{33}$$

From the symplectic property of the state transition matrix of Hamiltonian system, $\phi_{pp}(t_0, t)$ is given by $\phi_{pp}(t_0, t) = \phi_{xx}^{-T}$. Therefore ϕ_{pp} is explicitly given by

$$\phi_{pp} = \begin{bmatrix} \cos(\omega t) & -\frac{1}{\omega}\sin(\omega t) \\ \omega \sin(\omega t) & \cos(\omega t) \end{bmatrix}$$

From Eq. (32), the grammian and the inverse of the grammian are obtained as

$$W_c(t) = \begin{bmatrix} \frac{1}{\omega^2}\left(\frac{t}{2} - \frac{\sin(2\omega t)}{4\omega}\right) & \frac{\cos(2\omega t)}{4\omega^2} \\ \frac{\cos(2\omega t)}{4\omega^2} & \frac{t}{2} + \frac{\sin(2\omega t)}{4\omega} \end{bmatrix}, \; W_c^{-1}(t) = \begin{bmatrix} \frac{4\omega^3[2\omega t + \sin(2\omega t)]}{-1+4\omega^2 t^2} & -\frac{4\omega^2\cos(2\omega t)}{-1+4\omega^2 t^2} \\ -\frac{4\omega^2\cos(2\omega t)}{-1+4\omega^2 t^2} & \frac{4\omega[2\omega t - \sin(2\omega t)]}{-1+4\omega^2 t^2} \end{bmatrix}$$

Now, consider the asymptotic behavior of W_c^{-1} as as $t_f \to \infty$, which defines the attractive set for infinite time problem. It can be seen that as $t \to \infty$

$$\lim_{t\to\infty} W_c^{-1}(t) = \begin{bmatrix} 0 & 0 \\ 0 & 0 \end{bmatrix}$$

This implies $\lim_{t\to\infty} J^* = 0$ regardless of initial state and the attractive set is unbounded.

(ii) Degenerate Motion: $\alpha = 0$

In a similar way, ϕ_{xx} and ϕ_{pp} are given by

$$\phi_{xx} = \begin{bmatrix} 1 & t \\ 0 & 1 \end{bmatrix}, \; \phi_{pp} = \begin{bmatrix} 1 & 0 \\ -t & 1 \end{bmatrix}$$

Then, the grammian and the inverse of the grammian are obtained as

$$W_c(t) = \begin{bmatrix} \frac{t^3}{3} & -\frac{t^2}{2} \\ -\frac{t^2}{2} & t \end{bmatrix}, \; W_c^{-1}(t) = \begin{bmatrix} \frac{12}{t^3} & \frac{6}{t^2} \\ \frac{6}{t^2} & \frac{4}{t} \end{bmatrix}$$

Therefore the attractive set for infinite time problem is defined by

$$\lim_{t\to\infty} W_c^{-1}(t) = \begin{bmatrix} 0 & 0 \\ 0 & 0 \end{bmatrix}$$

For the degenerate case, the attractive set is unbounded as in the oscillatory case.

(iii) Hyperbolic Motion: $\alpha = -\lambda^2 < 0$

For the hyperbolic case, consider the transformation:

$$x = Tz, \;\; \bar{A} = T^{-1}AT = \begin{bmatrix} -\lambda & 0 \\ 0 & \lambda \end{bmatrix}$$

The transformation matrix is given by

$$T = \begin{bmatrix} -1 & 1 \\ \lambda & \lambda \end{bmatrix} \triangleq \begin{bmatrix} \boldsymbol{u}_- & \boldsymbol{u}_+ \end{bmatrix}$$

where $\boldsymbol{u}_-$, $\boldsymbol{u}_+$ correspond to stable and unstable eigenvectors. Moreover, the left eigenvectors of A are given by

$$\boldsymbol{v}_- = \frac{1}{2}\begin{bmatrix} -\lambda \\ 1 \end{bmatrix}, \; \boldsymbol{v}_+ = \frac{1}{2}\begin{bmatrix} \lambda \\ 1 \end{bmatrix} \tag{34}$$

Then ϕ_{xx} and ϕ_{pp} are given by

$$\bar{\phi}_{xx} = e^{-\bar{A}^T t} = \begin{bmatrix} e^{-\lambda t} & 0 \\ 0 & e^{\lambda t} \end{bmatrix}, \; \bar{\phi}_{pp} = e^{-\bar{A}^T t} = \begin{bmatrix} e^{\lambda t} & 0 \\ 0 & e^{-\lambda t} \end{bmatrix}$$

Then, $\bar{W}_c$ and $\bar{W}_c^{-1}$ are obtained as

$$\bar{W}_c(t) = \begin{bmatrix} \frac{-1+e^{2\lambda t}}{8\lambda} & \frac{t}{4} \\ \frac{t}{4} & -\frac{-1+e^{2\lambda t}}{8\lambda} \end{bmatrix}, \;\; \bar{W}_c^{-1}(t) = \begin{bmatrix} \frac{8\lambda(-1+e^{2\lambda t})}{1+e^{4\lambda t}-2e^{2\lambda t}(1+2t^2\lambda^2)} & -\frac{16\lambda^2 t e^{2\lambda t}}{1+e^{4\lambda t}-2e^{2\lambda t}(1+2t^2\lambda^2)} \\ -\frac{16\lambda^2 t e^{2\lambda t}}{1+e^{4\lambda t}-2e^{2\lambda t}(1+2t^2\lambda^2)} & \frac{8\lambda e^{2t\lambda}(-1+e^{2\lambda t})}{1+e^{4\lambda t}-2e^{2\lambda t}(1+2t^2\lambda^2)} \end{bmatrix}$$

Now, consider the asymptotic behavior of W_c^{-1} as as $t_f \to \infty$. It can be seen that as $t_f \to \infty$

$$\lim_{t\to\infty} \bar{W}_c^{-1}(t) = \begin{bmatrix} 0 & 0 \\ 0 & 8\lambda \end{bmatrix}$$

For the original system, the inverse of the grammian as $t \to \infty$ becomes

$$\lim_{t\to\infty} W_c^{-1}(t) = T^{-T}\begin{bmatrix} 0 & 0 \\ 0 & 8\lambda \end{bmatrix} T^{-1} = 2\lambda^2 \begin{bmatrix} \lambda & 1 \\ 1 & \frac{1}{\lambda} \end{bmatrix}$$

Therefore the optimal cost only depends on the unstable component of state z_u:

$$J^* = \frac{1}{2}\boldsymbol{x}^T W_c^{-1}\boldsymbol{x} = \frac{1}{2}\boldsymbol{z}^T \bar{W}_c^{-1}\boldsymbol{z} = 4\lambda z_u^2$$

The eigenvalues and corresponding (right) eigenvectors of $W_c^{-1}(\infty)$ are obtained as

$$\sigma = 0, \;\; \boldsymbol{u} = \begin{bmatrix} -1 \\ \lambda \end{bmatrix}, \tag{35}$$

$$\sigma = 2\lambda(1+\lambda^2), \;\; \boldsymbol{u} = \begin{bmatrix} \lambda \\ 1 \end{bmatrix} \tag{36}$$

Thus the attractive set is unbounded along the stable eigenvector $\boldsymbol{u}_-$ and the minimum extent is along the left eigenvector of unstable manifold $\boldsymbol{v}_+$.

4.2 Hill three-body problem

Hill's three-body problem is a simplification of the circular restricted three-body problem by assuming the first body has a larger mass than the second one and the third one has negligible mass [25]. It is in general a good model for approximating motion in the vicinity of the Earth for the spacecraft-Earth-Sun problem. The equations of motion in normalized form are given by

$$\ddot{X} - 2\dot{Y} = \frac{\partial V}{\partial x} \tag{37}$$

$$\ddot{Y} + 2\dot{X} = \frac{\partial V}{\partial y} \tag{38}$$

$$\ddot{Z} = \frac{\partial V}{\partial z} \tag{39}$$

$$V = \frac{\mu}{r} + \frac{1}{2}(3X^2 - Z^2),\ r = \sqrt{X^2 + Y^2 + Z^2} \tag{40}$$

where the coordinate system is centered on the second body [26]. The Hill problem has two equilibrium solutions, the libration point located at $X = \pm\left(\frac{1}{3}\right)^{1/3}, Y = Z = 0$.

The linearized equation about the equilibrium points is given by

$$\dot{x} = Ax + Bu \tag{41}$$

$$x = \begin{bmatrix} X & Y & Z & \dot{X} & \dot{Y} & \dot{Z} \end{bmatrix}^T,\ u = \begin{bmatrix} u_X & u_Y & u_Z \end{bmatrix}^T$$

$$A = \begin{bmatrix} 0 & 0 & 0 & 1 & 0 & 0 \\ 0 & 0 & 0 & 0 & 1 & 0 \\ 0 & 0 & 0 & 0 & 0 & 1 \\ 9 & 0 & 0 & 0 & 2 & 0 \\ 0 & -3 & 0 & -2 & 0 & 0 \\ 0 & 0 & -4 & 0 & 0 & 0 \end{bmatrix},\ B = \begin{bmatrix} 0 & 0 & 0 \\ 0 & 0 & 0 \\ 0 & 0 & 0 \\ 1 & 0 & 0 \\ 0 & 1 & 0 \\ 0 & 0 & 1 \end{bmatrix} \tag{42}$$

The eigenvalues of A are given by

$$\lambda_{1,2} = \pm\sqrt{2\sqrt{7} + 1} \tag{43}$$

$$\lambda_{3,4} = \pm j\sqrt{2\sqrt{7} - 1} \tag{44}$$

$$\lambda_{5,6} = \pm 2j \tag{45}$$

The first four eigenvalues $\lambda_{1,2}$ and $\lambda_{3,4}$, correspond to the in-plane motion while the eigenvalues $\lambda_{5,6}$ correspond to the out of plane motion. Note that the out-of-plane motion is decoupled in the linearized equation and consists only of periodic motions while the in-plane motion consists of a stable, an unstable and a center manifold.

4.2.1 Attractive set of equilibrium point

For the planar motion of Eq. (41), the attractive set of optimal control to transfer to the equilibrium point is considered. Consider the transformation

$$x = Tz, \;\; z^T = \begin{bmatrix} z_s & z_u & z_{c1} & z_{c2} \end{bmatrix}$$

Then the in-plane motion of Eq. (41) becomes

$$\dot{z} = \bar{A}z + \bar{B}u, \quad z(0) = T^{-1}x_0, \;\; z(t_f) = 0 \tag{46}$$

where

$$\bar{A} = T^{-1}AT = \left[\begin{array}{cc|cc} -\lambda & & & \mathbf{0} \\ & \lambda & & \\ \hline & & 0 & -\omega \\ \mathbf{0} & & \omega & 0 \end{array}\right], \quad \bar{B} = T^{-1}B \tag{47}$$

$$\lambda = \sqrt{2\sqrt{7}+1}, \;\; \omega = \sqrt{2\sqrt{7}-1} \tag{48}$$

The attractive set to transfer to the origin was computed by Lyapunov difference equation (13) over a time interval $[0, t_f]$ in nondimensional time. We choose to plot attractive sets in the plane of intersection of the stable and unstable eigenvectors with the x-axis aligned with the left unstable eigenvector and y-axis with the right stable eigenvector. This new manifold coordinates (X_m-Y_m) is shown in Fig. 1. Figure 2 shows the projection of attractive sets into X-Y plane for the finite time ($t_f = 15, 30, 100$) and infinite time case, respectively. Each line represents the surface of the attractive sets with the same cost. As the time of flight increases, the attractive region becomes larger and finally becomes unbounded along the right stable eigenvector as is developed analytically in Section 2. From Lemma 3.1, the limit of the inverse of the grammian exists and given by

$$\bar{W}_c^{-1}(\infty) = T^T W_c^{-1}(\infty) T = \begin{bmatrix} 0 & 0 & 0 & 0 \\ 0 & p^{-1} & 0 & 0 \\ 0 & 0 & 0 & 0 \\ 0 & 0 & 0 & 0 \end{bmatrix} \tag{49}$$

where p is solution to the scalar Lyapunov equation:

$$(-\lambda)p + p(-\lambda) + b_2 b_2^T = 0 \tag{50}$$

and is given by $p = b_2 b_2^T / 2\lambda$, hence $p^{-1} = 2\lambda / b_2 b_2^T \approx 13.467$. Then, $W_c^{-1}(\infty)$ is expressed in terms of the unstable eigenvalue λ and the left unstable eigenvector $\boldsymbol{v}_+$ associated with A as

$$W_c^{-1}(\infty) = p^{-1} \boldsymbol{v}_+ \boldsymbol{v}_+^T$$

Figure 3 illustrates the optimal trajectories projected into X_m-Y_m plane for $t_f = 5, 1000$ respectively. For the long time duration case, the optimal control is known to be extremely sensitive to the numerical error. Therefore, the transient behavior of $W_c^{-1}(t, 0)$ is ignored and the constant feedback gain is used in the simulation. Figure 4 shows the corresponding trajectories in the manifold coordinates.

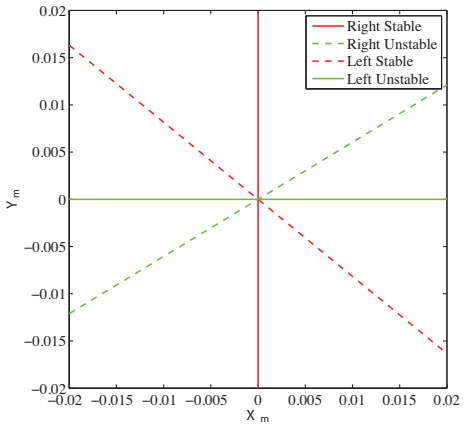

Fig. 1: New coordinate system: the left stable eigenvector is perpendicular to the right unstable eigenvector in the full 6-D space but not in the current projection.

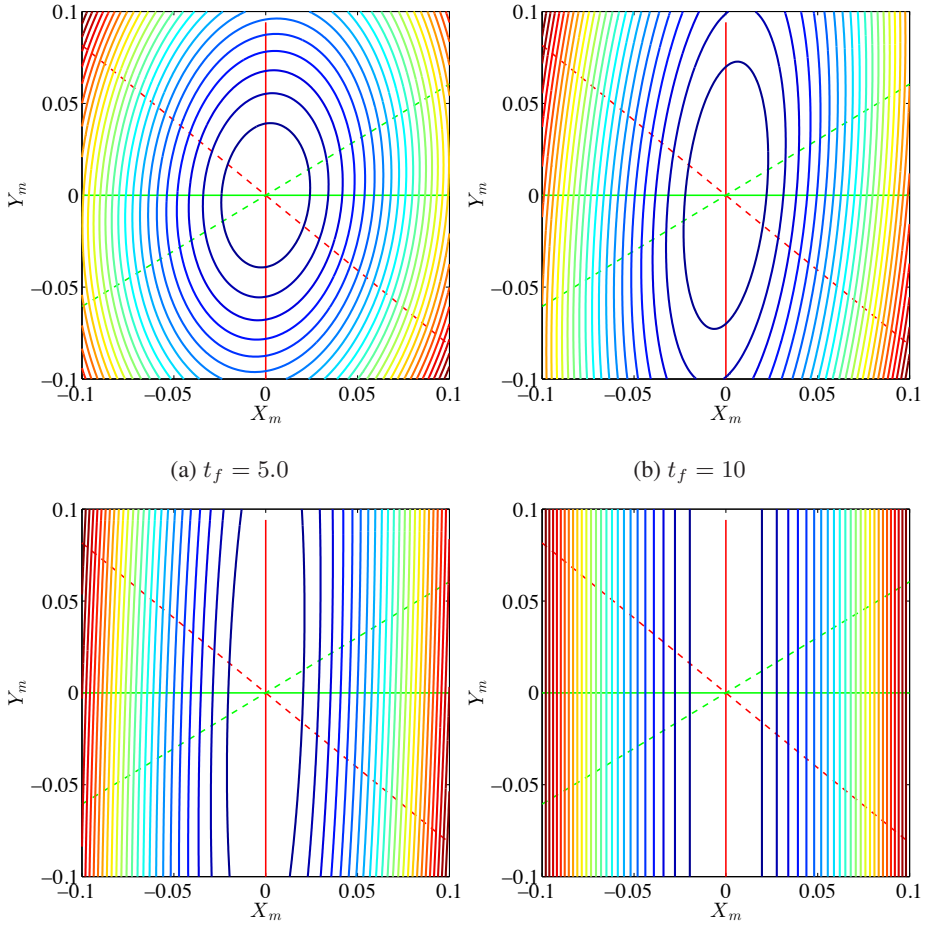

(a) $t_f = 5.0$ (b) $t_f = 10$

(c) $t_f = 100$ (d) $t_f = \infty$

Fig. 2: Attractive set of L_2 point for different times of flight.

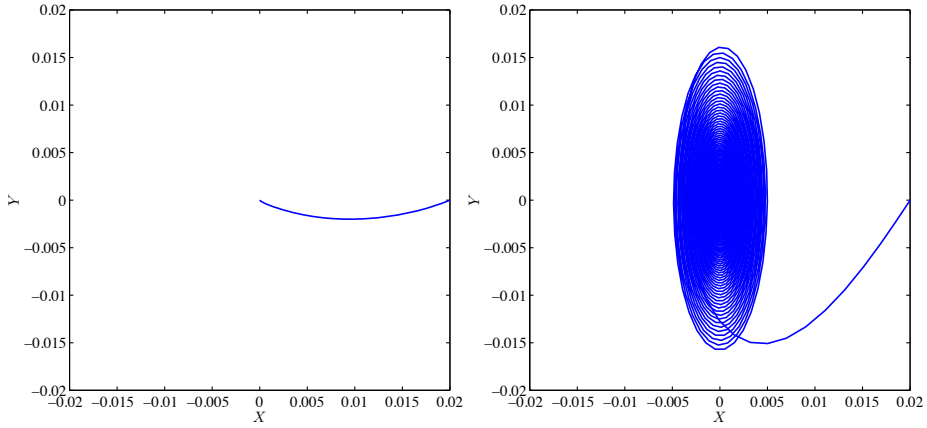

(a) $t_f = 5.0$ (b) $t_f = 1000$

Fig. 3: Optimal trajectories for different times of flight.

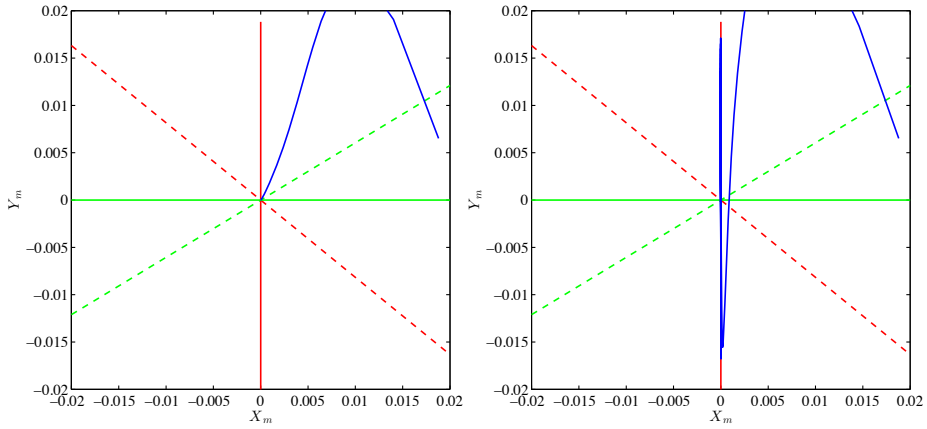

(a) $t_f = 5.0$ (b) $t_f = 1000$

Fig. 4: Optimal trajectories for different times of flight in the manifold coordinates.

4.2.2 Attractive set of a fixed point: Lyapunov orbit case

Next, the optimal control problem to transfer to a periodic orbit in the vicinity of the libration point is considered. In this case, the attractive set is defined as the set of all initial states in which the optimal control can drive the state to the desired point on the final periodic orbit. In this example, we consider a planar periodic orbit solution of the Hill's problem. The particular Lyapunov orbit is given by the normalized initial condition

$$x_{ref}(0) = \begin{bmatrix} 0.7000 & 0.0000 & -0.3979 & 0.0000 & -0.04449 & 0.0000 \end{bmatrix}^T$$

and its period is $T = 3.0332$. Figure 5 shows this Lyapunov orbit. This orbit is unstable with characteristic exponents $\sigma = \pm 2.0121$.

The linearized equation along x_{ref} is given by

$$\dot{x} = A(t)x + Bu \tag{51}$$

where

$$A(t) = \left[\begin{array}{c|c} 0 & I \\ \hline \frac{\partial^2 V}{\partial^2 r} & 2J \end{array}\right]_{\boldsymbol{x}=\boldsymbol{x}_{ref}}$$

$$= \begin{bmatrix} 0 & 0 & 0 & 1 & 0 & 0 \\ 0 & 0 & 0 & 0 & 1 & 0 \\ 0 & 0 & 0 & 0 & 0 & 1 \\ 3+\frac{3X^2}{r^5}-\frac{1}{r^3} & \frac{3XY}{r^5} & \frac{3XZ}{r^5} & 0 & 2 & 0 \\ \frac{3XY}{r^5} & \frac{3Y^2}{r^5}-\frac{1}{r^3} & \frac{3YZ}{r^5} & -2 & 0 & 0 \\ \frac{3XZ}{r^5} & \frac{3YZ}{r^5} & -1+\frac{3Z^2}{r^5}-\frac{1}{r^3} & 0 & 0 & 0 \end{bmatrix}_{x=x_{ref}}$$

Note that $A(t)$ is T-periodic function of time.

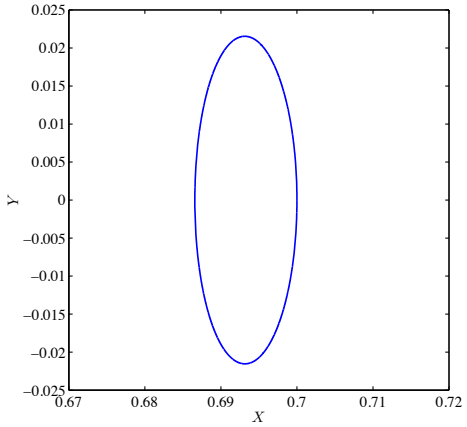

Fig. 5: Lyapunov orbit.

As shown in Appendix B, the grammian $W_c(t,0)$ can be divided into two part: the grammian from $t=0$ to $t=kT$, and the grammian from $t=kT$ to t_f. For simplicity, we assume that the desired state is on the same Poincaré section of the initial state, i.e., $t_f = k_f T$. From Lemma 3.2, W_c^{-1} as $k_f \to \infty$ is given by

$$\lim_{t\to\infty} W_c^{-1}(t,0) = \lim_{k\to\infty} Y^{-1}(k) = \begin{bmatrix} 0 & 0 & 0 & 0 & 0 & 0 \\ 0 & p^{-1} & 0 & 0 & 0 & 0 \\ 0 & 0 & 0 & 0 & 0 & 0 \\ 0 & 0 & 0 & 0 & 0 & 0 \\ 0 & 0 & 0 & 0 & 0 & 0 \\ 0 & 0 & 0 & 0 & 0 & 0 \end{bmatrix} \tag{52}$$

where $p \approx 27.86$ is solution to the Lyapunov equation:

$$(e^{\sigma T})^2 p + \left(\int_0^T \phi_{11}^T(\tau, t_0) B_1 B_1^T \phi_{11}(\tau, t_0) d\tau \right) = 0 \tag{53}$$

where σ is the unstable characteristic exponent of the Lyapunov orbit. The attractive set for the finite-time problem is obtained by solving the difference Lyapunov equation (16) over $[0, k_f]$ and approaches the limit which is analytically predicted in Eq. (52). In the manifold coordinates, the attractive region becomes larger and finally becomes unbounded along the right stable eigenvector as in the previous example. Figure 6 illustrates the optimal trajectories projected into X_m-Y_m plane for $t_f = 5T,\ 50T$ respectively. As in the equilibrium case, optimal control is very sensitive to numerical error for the long time duration case. Therefore, the transient behavior of $W_c^{-1}(t,0)$ is ignored and the periodic feedback gain is used in the simulation. Figure 7 (a) and 7 (b) show the corresponding trajectories in the manifold coordinates for Fig. 6. In the manifold coordinates, the optimal trajectories first approach the Y_m-axis (stable manifold) and the converges to the origin along Y_m-axis. Figure 7 (c) and 7 (d) show the trajectories for increasing k_f. It is interesting to note that the point to intersect Y_m-axis converges to a certain point which is the limit point for the first iteration in the infinite time case as

$$\begin{aligned} z(T) &= e^{MT} z(0) - e^{MT} \left(\int_0^T \phi_{pp}^{-T}(\tau, 0) B B^T \phi_{pp}(\tau, 0) d\tau \right) Y^{-1}(\infty) z(0) \\ &= \begin{bmatrix} e^{\sigma_s T} z_s(0) \\ 0 \\ e^{\sigma_c T} z_c(0) \end{bmatrix} \end{aligned}$$

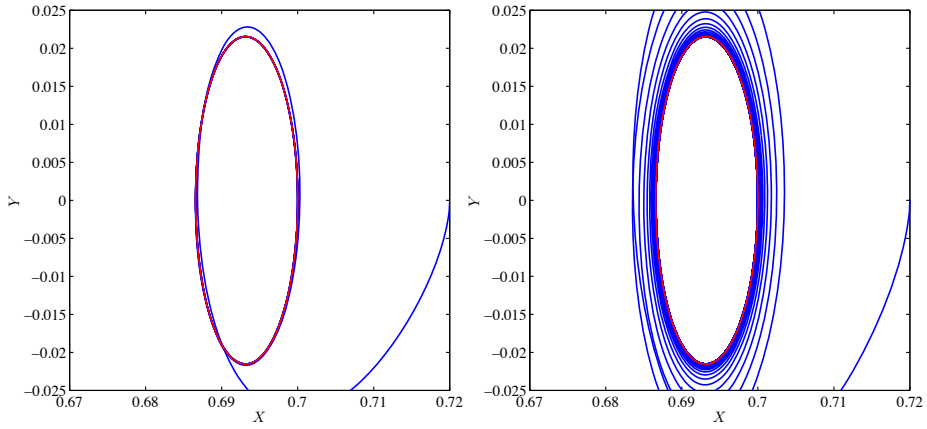

(a) $t_f = 5T$ (b) $t_f = 50T$

Fig. 6: Optimal trajectories.

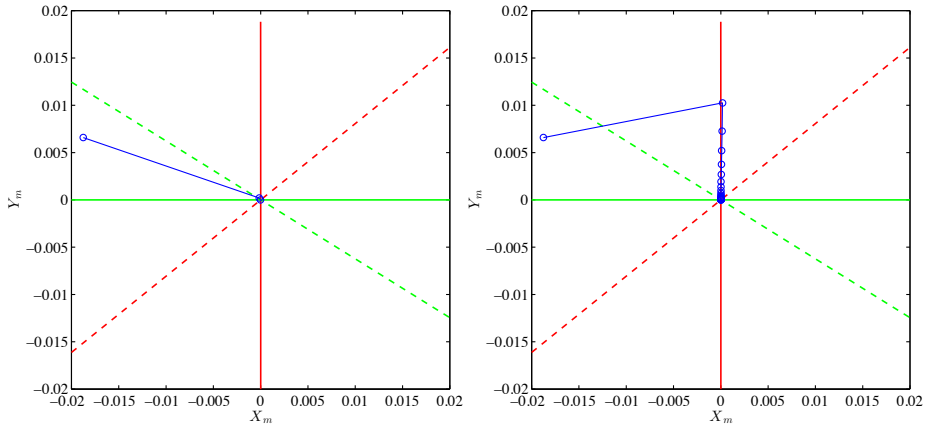

(a) $k_f = 5$. (b) $k_f = 50$.

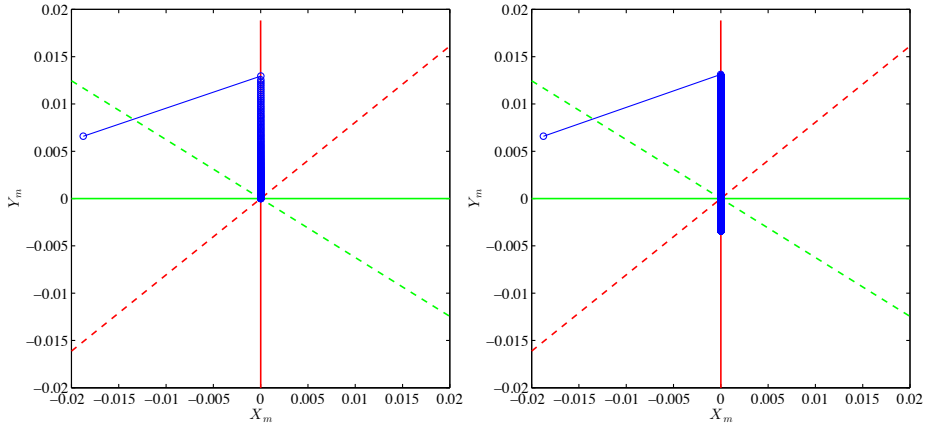

(c) $k_f = 1000$. (d) $k_f = 10000$.

Fig. 7: Optimally controlled trajectories projected into the manifold coordinates: the solid red, dotted green, solid green, and dotted red lines are aligned with right stable, right unstable, left unstable and left stable eigenvectors.

4.2.3 Attractive set of a fixed point: the halo orbit case

The attractive set for the three-dimensional periodic orbit called halo orbit is now considered. Halo orbits are found by continuation from their bifurcation from planar Lyapunov orbits [26]. The particular halo orbit is given by the normalized initial condition

$$x_{ref}(0) = \begin{bmatrix} 0.7406 & 0.0000 & 0.0000 & 0.0000 & -0.8509 & 0.0000 \end{bmatrix}^T$$

and its period is $T = 3.0461$. Figure 8 depicts this halo orbit in 3-dimensional position space, projection into $X - Y$ plane, $Y - Z$ plane and $X - Z$ plane. This halo orbit has one pair of hyperbolic characteristic exponents $\sigma = \pm 6.5918$ and a four dimensional center manifold.

Then $\bar{W}_c^{-1}$ as $t \to \infty$ becomes

$$\lim_{t\to\infty} \bar{W}_c^{-1}(t,0) = \lim_{k\to\infty} \bar{Y}^{-1}(k) = \begin{bmatrix} 0 & 0 & 0 & 0 & 0 & 0 \\ 0 & p^{-1} & 0 & 0 & 0 & 0 \\ 0 & 0 & 0 & 0 & 0 & 0 \\ 0 & 0 & 0 & 0 & 0 & 0 \\ 0 & 0 & 0 & 0 & 0 & 0 \\ 0 & 0 & 0 & 0 & 0 & 0 \end{bmatrix} \tag{54}$$

where $p \approx 16.563$ is the solution to the Lyapunov equation:

$$(e^{\sigma T})^2 p + \left(\int_0^T \phi_{11}^T(\tau, t_0) B_1 B_1^T \phi_{11}(\tau, t_0) d\tau \right) = 0 \tag{55}$$

where σ is the unstable characteristic exponent of the halo orbit. The attractive set for the finite-time problem is obtained by solving the difference Lyapunov equation (16) over $[0, k_f]$ and approaches the limit which is analytically predicted in Eq. (52). In the manifold coordinates, the attractive region becomes larger and finally become unbounded along the right stable eigenvector as in the previous examples. Figure 9 shows the eigenvalues of $Y(k)$ as a function of $\log(k_f)$. From Fig. 9, it can be confirmed that λ_2 converges to a constant (≈ 16) while the other eigenvalues converges to zero. The optimal controlled trajectory is shown in Figs. 10 and 11 where $k_f = 5 (t_f = 5T)$ and $k_f = 1000 (t_f = 1000T)$ respectively. As in the Lyapunov orbit case, the transient behavior of $W_c^{-1}(t, 0)$ is ignored and the periodic feedback gain is used in the simulation. Figure 12 shows the optimally controlled trajectory in the manifold coordinates for $k_f = 5, 100, 1000, 10000$. One can find that the optimally controlled trajectories are similar to those of the Lyapunov orbit case in the manifold coordinates.

The linear control laws were also tested in the full nonlinear equations of motion (37)-(39). Figure 13 shows that for short-time ($k_f = 10$) the linear results would drive the trajectory to the periodic orbit, clearly following the dynamical structure For long-term iterates ($k_f = 1000$) the instability of the problem overpowers the weak thrusting, and the trajectory controlled with the linear control law eventually diverges (fixes are available but were not applied).

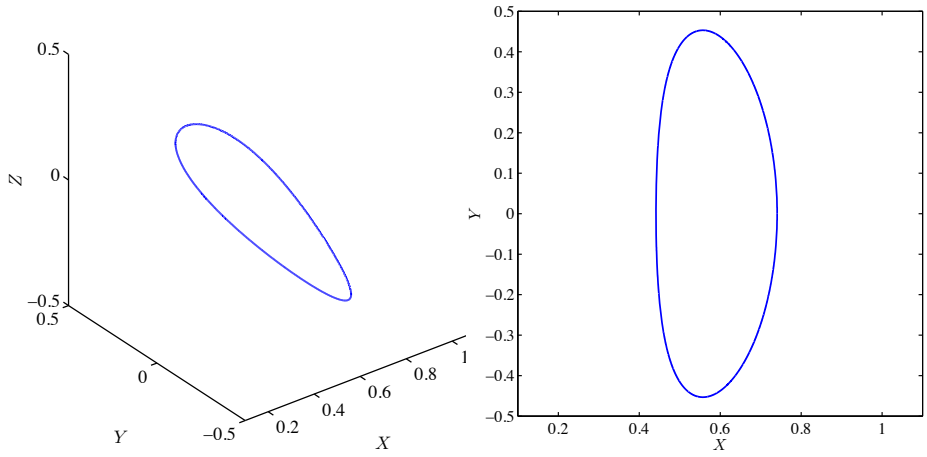

(a) 3D trajectory.

(b) Projection into the X-Y plane.

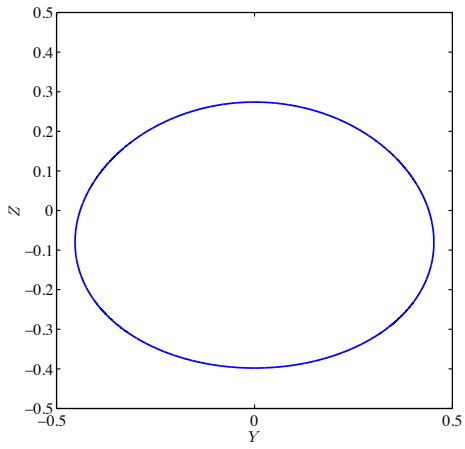

(c) Projection into the Y-Z plane.

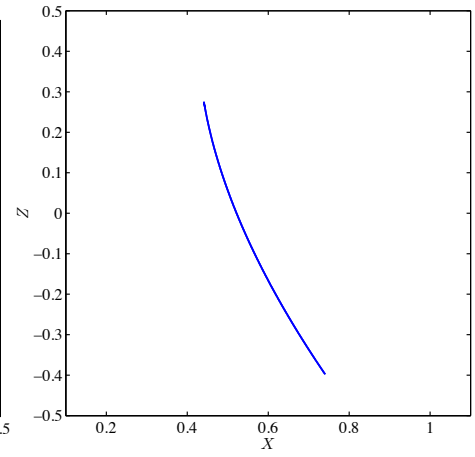

(d) Projection into the X-Z plane.

Fig. 8: Halo orbit.

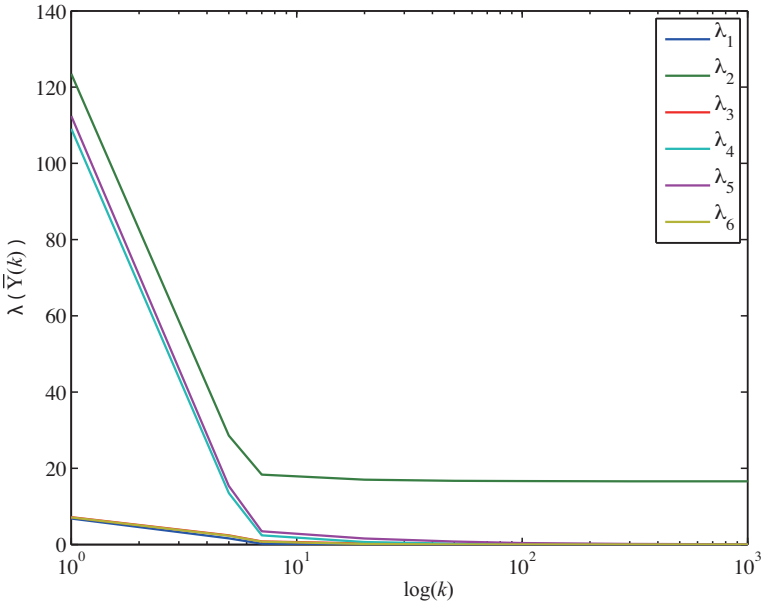

Fig. 9: Eigenvalues of $Y(k)$.

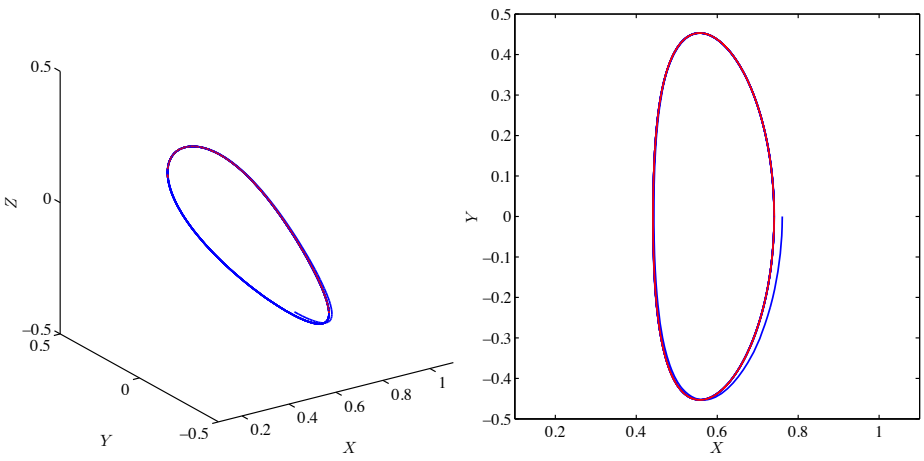

(a) 3D trajectory.

(b) Projection into the X-Y plane.

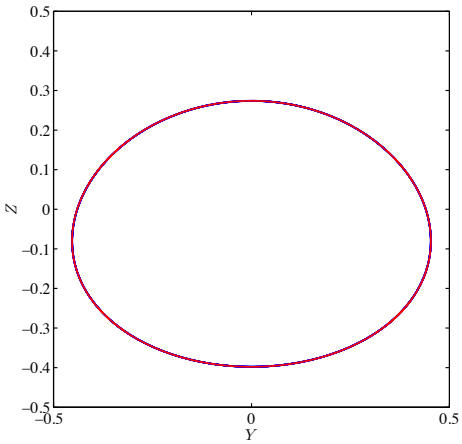

(c) Projection into the Y-Z plane.

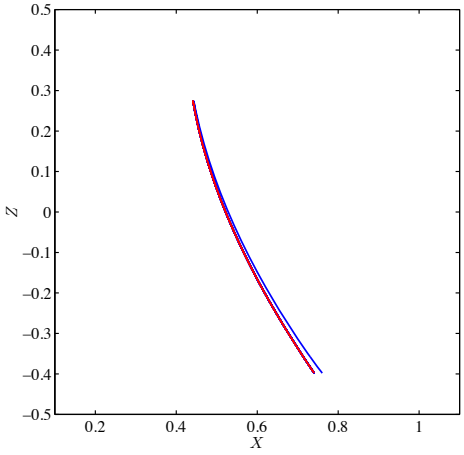

(d) Projection into the X-Z plane.

Fig. 10: Optimal controlled trajectory for $t_f = 5T$.

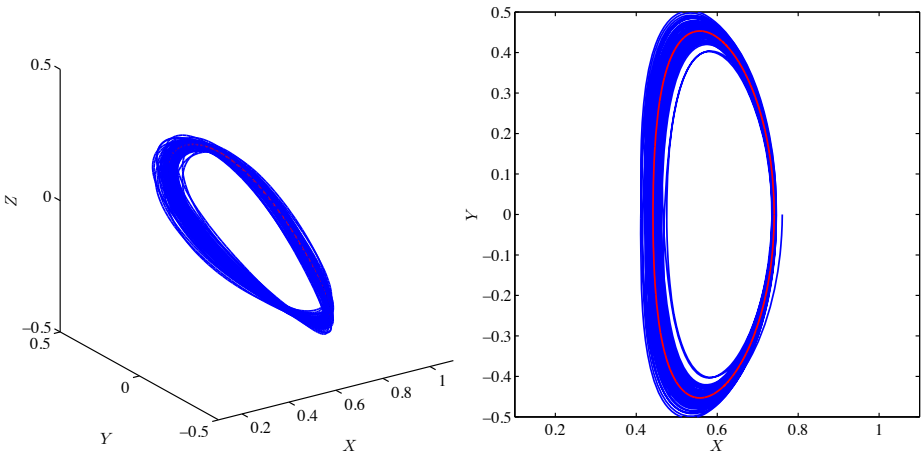

(a) 3D trajectory.

(b) Projection into the X-Y plane.

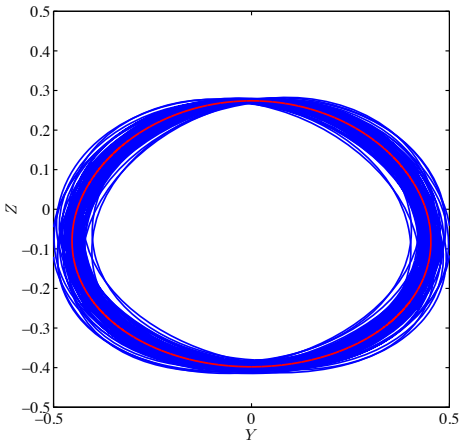

(c) Projection into the Y-Z plane.

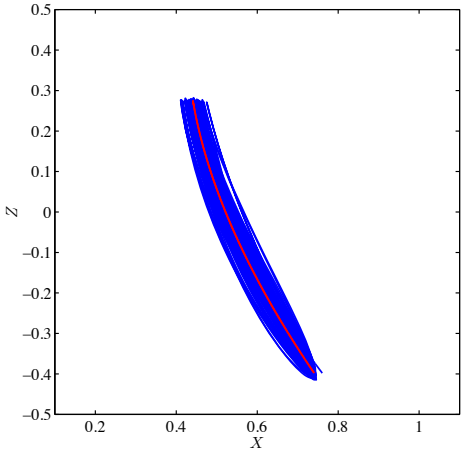

(d) Projection into the X-Z plane.

Fig. 11: Optimal controlled trajectory for $t_f = 1000T$.

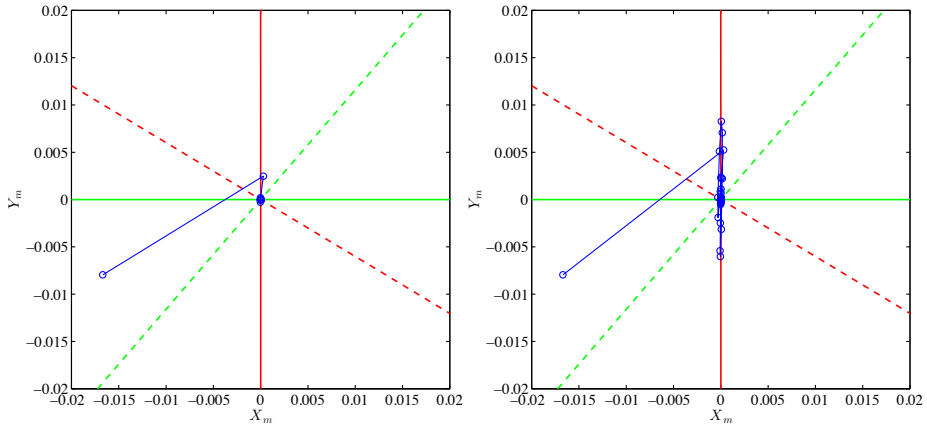

(a) $k_f = 5$. (b) $k_f = 100$.

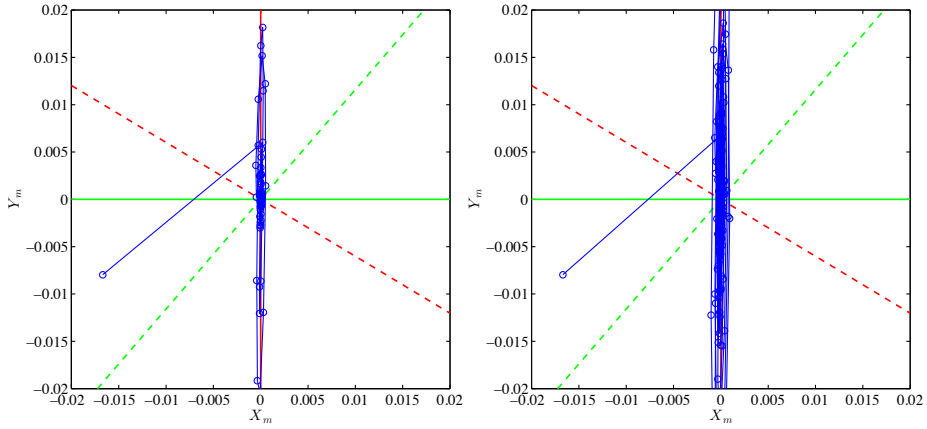

(c) $k_f = 1000$. (d) $k_f = 10000$.

Fig. 12: Optimally controlled trajectories projected into the manifold coordinates: the solid red, dotted green, solid green, and dotted red lines are aligned with right stable, right unstable, left unstable and left stable eigenvectors.

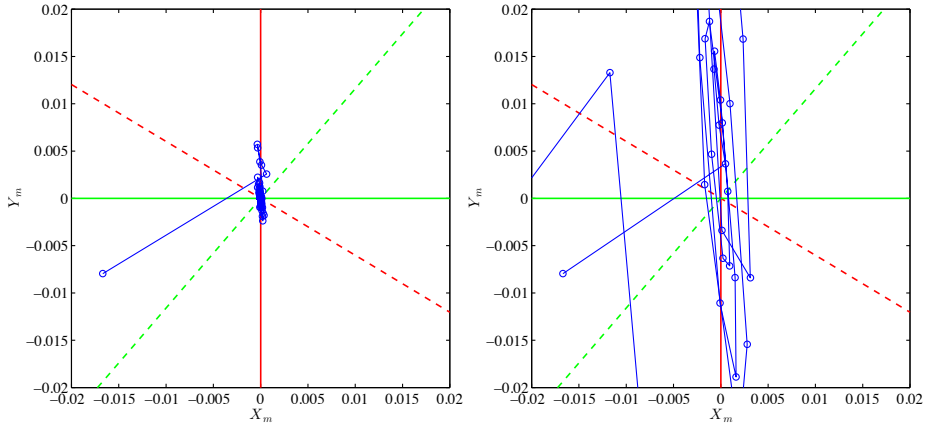

(a) $k_f = 100$. (b) $k_f = 1000$.

Fig. 13: Optimally controlled trajectories projected into the manifold coordinates for the full nonlinear equations of motion. Note $k_f = 100$ converges and $k_f = 1000$ diverges from the orbit eventually.

5 Conclusions

This paper presents the basic properties of the attractive set of optimal feedback control to dynamical systems in astrodynamics problems. The combination of optimal feedback control with the dynamical structure of the three-body problem yields a direct relation between the attractive set and the dynamical structure of the original system. In particular we find that the largest dimensions of the set are found along the stable manifold and the least extent is along the left eigenvector of the unstable manifold. A simple 1-DOF system is used to illustrate the theory. Then we demonstrate the theory through optimal transfer problem in Hill's three-body problem. This approach enables a new class of missions, whose solutions are not obtainable neither through the patched-conics method nor through the classic invariant manifolds technique. Knowledge of this relationship has the potential to be very useful in determining initial guesses and control laws for these optimization algorithms.

Appendix A: Proof of Lemma 3.1

Consider the transformation

$$\boldsymbol{x} = T\boldsymbol{z}, \quad \boldsymbol{z}^T = \begin{bmatrix} \boldsymbol{z}_u & \boldsymbol{z}_s & \boldsymbol{z}_c \end{bmatrix}$$

$$\bar{A} = T^{-1}AT = \begin{bmatrix} A_u & & 0 \\ & A_s & \\ 0 & & A_c \end{bmatrix}, \quad \bar{B} = T^{-1}B$$

Note that the order of submatrices are different from Eq. (19). By using the new variable z, the optimal cost is given by

$$\begin{aligned} J^* &= \frac{1}{2}x_0^T W_c^{-1} x_0 \\ &= \frac{1}{2}z_0^T (T^T W_c^{-1}(t) T) z_0 \\ &= \frac{1}{2}z_0^T \bar{W}_c^{-1}(t) z_0 \end{aligned} \tag{56}$$

where

$$\begin{aligned} \bar{W}_c^{-1}(t) &= T^T W_c^{-1}(t) T \\ &= \left(\int_{t_0}^{t} (T^{-1}e^{-At}T)T^{-1}BB^T T^{-T}(T^T e^{-A^T t}T^{-T})dt \right)^{-1} \\ &= \left(\int_{t_0}^{t} e^{-\bar{A}t}\bar{B}\bar{B}^T e^{-\bar{A}^T t} dt \right)^{-1} \end{aligned} \tag{57}$$

Now consider $\bar{W}_c^{-1}(t) = \left(\int_{t_0}^{t} e^{-\bar{A}t}\bar{B}\bar{B}^T e^{-\bar{A}^T t}dt\right)^{-1}$ when $t \to \infty$. It can be found that $\bar{W}_c$ is the controllability grammian of $(-\bar{A}, \bar{B})$. Since the system (A, B) is controllable, $\bar{W}_c(t)$ is positive definite for $t > 0$. Moreover, $\bar{W}_c(t)$ is the solution of the following differential equation

$$\dot{\bar{W}}_c = (-\bar{A})\bar{W}_c + \bar{W}_c(-\bar{A}^T) + \bar{B}\bar{B}^T, \;\; \bar{W}_c(0) = \mathbf{0} \tag{58}$$

If we define

$$(-\bar{A}) = \left[\begin{array}{c|c} A_1 & \mathbf{0} \\ \hline \mathbf{0} & A_2 \end{array}\right] = \left[\begin{array}{c|cc} -A_u & 0 & 0 \\ \hline 0 & -A_s & 0 \\ 0 & 0 & -A_c \end{array}\right], \quad \bar{B} = \left[\begin{array}{c} B_1 \\ B_2 \end{array}\right] = \left[\begin{array}{c} B_u \\ \hline B_s \\ B_c \end{array}\right]$$

$$\bar{W}_c(t) = \left[\begin{array}{c|c} W_{11} & W_{12} \\ \hline W_{21} & W_{22} \end{array}\right]$$

then Eq. (58) is decomposed into

$$\dot{W}_{11} = A_1 W_{11} + W_{11}A_1^T + B_1 B_1^T, \;\; \bar{W}_{11}(0) = \mathbf{0} \tag{59}$$

$$\dot{W}_{12} = A_1 W_{12} + W_{12}A_2^T + B_1 B_2^T, \;\; \bar{W}_{12}(0) = \mathbf{0} \tag{60}$$

$$\dot{W}_{22} = A_2 W_{22} + W_{22}A_2^T + B_2 B_2^T, \;\; \bar{W}_{22}(0) = \mathbf{0} \tag{61}$$

Note that A_1 and A_2 are stable and unstable submatrix of $-\bar{A}$. Since $\bar{W}_c(t) = \left(\int_{t_0}^{t} e^{-\bar{A}t}\bar{B}\bar{B}^T e^{-\bar{A}^T t}dt\right) \geq 0$ is symmetric, $W_{12}(t) = W_{21}(t)$. The inverse of $\bar{W}_c(t)$ is given by

$$\bar{W}_c^{-1}(t) = \left[\begin{array}{cc} W_{11}^{-1} + W_{11}^{-1}W_{12}S^{-1}W_{21}W_{11}^{-1} & -W_{11}^{-1}W_{12}Z_{22}^{-1} \\ -Z_{22}^{-1}W_{21}W_{11}^{-1} & S^{-1} \end{array}\right] \triangleq \left[\begin{array}{cc} W_{11}^{-1} + Z_{11} & -Z_{12} \\ -Z_{21} & Z_{22} \end{array}\right]$$

$$S \triangleq W_{22} - W_{21}W_{11}^{-1}W_{12}$$

In the following, we verify Z_{11}, Z_{12}, $Z_{22} \to 0$ as $t \to \infty$.

(i) $Z_{22}(t)$

It is clear that $S(t) > 0$ since $W_c(t)$ and $W_c^{-1}(t)$ are positive definite for $t > 0$. Moreover, from Eq. (64) - (61), the following equation is obtained

$$\begin{aligned} \dot{S} &= \frac{d}{dt}(W_{22} - W_{21}W_{11}^{-1}W_{12}) \\ &= \dot{W}_{22} - \dot{W}_{21}W_{11}^{-1}W_{12} - W_{21}\dot{W}_{11}^{-1}W_{12} - W_{21}W_{11}^{-1}\dot{W}_{12} \\ &= A_2 S + S A_2 + (W_{21}W_{11}^{-1}B_1 - B_2)(W_{21}W_{11}^{-1}B_1 - B_2)^T \end{aligned} \tag{62}$$

Therefore $\dot{S} \geq 0$.Moreover, from the relation

$$\dot{S}^{-1} = -S^{-1}\,\dot{S}\,S^{-1} < 0 \tag{63}$$

it follows that $Z_{22}(t) = S^{-1}(t) \to 0$ as $t \to \infty$.

(ii) $Z_{12}(t)$**,** $Z_{21}(t)$

From Eq. (64) - (61), the following equation is obtained

$$\dot{Z}_{21} = -\left[A_2^T + Z_{22}(W_{21}W_{11}^{-1}B_1 - B_2)(W_{21}W_{11}^{-1}B_1 - B_2)^T\right] Z_{21} - Z_{21}(A_1 + B_1B_1^TW_{11}^{-1}) + Z_{22}B_2B_1^TW_{11}^{-1} \tag{64}$$

When t is sufficiently large, $Z_{22} \to 0$ and Eq. (64) becomes

$$\dot{Z}_{21} \approx -A_2^TZ_{21} - Z_{21}(A_1 + B_1B_1^TW_{11}^{-1}) \tag{65}$$

Now, we show $(A_1 + B_1B_1^TW_{11}^{-1})$ in Eq. (65) is positive definite. From Eq. (64), it follows that

$$\begin{aligned}
&\dot{W}_{11} = A_1W_{11} + W_{11}A_1^T + B_1B_1^T > 0 \\
\Rightarrow\ &\dot{W}_{11}^{-1} = -W_{11}^{-1}(A_1W_{11} + W_{11}A_1^T + B_1B_1^T)W_{11}^{-1} \\
&\qquad = -W_{11}^{-1}A_1 - A_1^TW_{11}^{-1} + W_{11}^{-1}B_1B_1^TW_{11}^{-1} \\
&\qquad = -W_{11}^{-1}(A_1 + B_1B_1^TW_{11}^{-1}) - (A_1 + B_1B_1^TW_{11}^{-1})^TW_{11}^{-1} + W_{11}^{-1}B_1B_1^TW_{11}^{-1} < 0
\end{aligned}$$

From the inequality of the last equation and $W_{11}^{-1} > 0$, $A_1 + B_1B_1^TW_{11}^{-1} > 0$. Therefore, $Z_{21},\ Z_{12} \to 0$.

(iii) $Z_{11}(t)$

From Eq. (64) - (61), the following equation is obtained

$$\dot{Z}_{11} = -(A_1 + B_1B_1^TW_{11}^{-1})^TZ_{11} - Z_{11}(A_1 + B_1B_1^TW_{11}^{-1}) + Z_{12}B_2B_1^TW_{11}^{-1} + W_{11}^{-1}B_1B_2^TZ_{21} - Z_{12}(W_{21}W_{11}^{-1}B_1 - B_2)(W_{21}W_{11}^{-1}B_1 - B_2)^TZ_{21} \tag{66}$$

When t is sufficiently large, $Z_{12}, Z_{21} \to 0$ and Eq. (66) becomes

$$\dot{Z}_{11} \approx -(A_1 + B_1B_1^TW_{11}^{-1})^TZ_{11} - Z_{11}(A_1 + B_1B_1^TW_{11}^{-1}) < 0 \tag{67}$$

Since $A_1 + B_1B_1^TW_{11}^{-1} > 0$, $Z_{11}(t) \to 0$.

From **(i)-(iii)**, we can see that

$$\lim_{t\to\infty} \bar{W}_c^{-1}(t) = \begin{bmatrix} W_{11}^{-1} & 0 \\ 0 & 0 \end{bmatrix} \tag{68}$$

where W_{11} is solution to the Lyapunov equation:

$$A_1^TW_{11} + W_{11}A_1 + B_1B_1^T = 0 \tag{69}$$

Finally, we have

$$\lim_{t\to\infty} \bar{W}_c^{-1}(t) = \bar{W}_c^{-1}(\infty) = \begin{bmatrix} 0 & 0 & 0 \\ 0 & W_{uu}^{-1} & 0 \\ 0 & 0 & 0 \end{bmatrix} \tag{70}$$

by rearranging the column vectors of transformation matrix T.

(vi) Eigenstructure of W_c^{-1}

$$\bar{W}_c^{-1}(\infty) = T^T W_c^{-1}(\infty) T = \begin{bmatrix} 0 & 0 & 0 \\ 0 & W_{uu}^{-1} & 0 \\ 0 & 0 & 0 \end{bmatrix} \tag{71}$$

Let $\boldsymbol{u}_i$ and $\boldsymbol{v}_i$ $(i = 1, \cdots n)$ be the right and left eigenvector corresponding to the eigenvalue λ_i respectively as defined in Eqs. (21) and (22). By substituting Eqs. (21) and (22) into (71), we have

$$\begin{aligned} W_c^{-1}(\infty) &= T^{-T} \begin{bmatrix} 0 & 0 & 0 \\ 0 & W_{uu}^{-1} & 0 \\ 0 & 0 & 0 \end{bmatrix} T^{-1} = T^{-T} \begin{bmatrix} 0 \\ W_{uu}^{-1} V_u \\ 0 \end{bmatrix} = \begin{bmatrix} V_s & V_u & V_c \end{bmatrix} \begin{bmatrix} 0 \\ W_{uu}^{-1} V_u \\ 0 \end{bmatrix} \\ &= V_u W_{uu}^{-1} V_u^T \end{aligned} \tag{72}$$

Appendix B: Proof of Lemma 3.2

Assume $t_0 = 0, kT \le t_f \le (k+1)T$. By application of Floquet's theorem [23], there exist a constant matrix M such that $\phi_{xx}(T, 0) = e^{MT}$. Then

$$\begin{aligned} W_c(t_f, 0) &= \int_0^{t_f} \phi_{pp}^T(\tau, 0) B B^T \phi_{pp}(\tau, 0) d\tau \\ &\quad + \int_{(k-1)T}^{kT} \phi_{pp}^T(\tau, 0) B B^T \phi_{pp}(\tau, 0) d\tau + \int_{kT}^{t} \phi_{pp}^T(\tau, 0) B B^T \phi_{pp}(\tau, 0) d\tau \\ &= \int_0^{T} \phi_{pp}^T(\tau, 0) B B^T \phi_{pp}(\tau, 0) d\tau + e^{-MT} \left(\int_0^{T} \phi_{pp}^T(\tau, 0) B B^T \phi_{pp}(\tau, 0) d\tau \right) e^{-M^T T} + \cdots \\ &\quad + e^{-MT(k-1)} \left(\int_0^{T} \phi_{pp}^T(\tau, 0) B B^T \phi_{pp}(\tau, 0) d\tau \right) e^{-M^T T(k-1)} + \int_{kT}^{t_f} \phi_{pp}^T(\tau, 0) B B^T \phi_{pp}(\tau, 0) d\tau \\ &= \sum_{j=0}^{k-1} e^{-MTj} \left(\int_0^{T} \phi_{pp}^T(\tau, 0) B B^T \phi_{pp}(\tau, 0) d\tau \right) e^{-M^T Tj} + \int_{kT}^{t_f} \phi_{pp}^T(\tau, 0) B B^T \phi_{pp}(\tau, 0) d\tau \end{aligned}$$

Replacing

$$\begin{aligned} e^{MT} &\to A \\ e^{-M^T T} &\to A^{-T} \\ \left(\int_0^{T} \phi_{pp}^T(\tau, 0) B B^T \phi_{pp}(\tau, 0) d\tau \right) &\to B B^T \\ \sum_{j=0}^{k-1} e^{-MTj} \left(\int_0^{T} \phi_{pp}^T(\tau, 0) B B^T \phi_{pp}(\tau, 0) d\tau \right) e^{-M^T Tj} &\to Y(k) \end{aligned}$$

and setting $t_f = kT$ then $Y(k)$ satisfies the Lyapunov difference equation

$$Y(k+1) = A^{-1} Y(k) A^{-T} + B B^T \tag{73}$$

This is easily verified by

$$\begin{aligned} Y(k+1) &= \sum_{j=1}^{k} (A^{-1})^j BB^T (A^{-T})^j + BB^T \\ &= A^{-1} \left(\sum_{j=0}^{k-1} (A^{-1})^j BB^T (A^{-T})^j \right) A^{-T} + BB^T \\ &= A^{-1} Y(k) A^{-T} + BB^T \end{aligned}$$

For $k \to \infty$, $Y(\infty) = \sum_{j=0}^{\infty} (A^{-1})^j BB^T (A^{-T})^j$ satisfies the Lyapunov equation

$$Y(\infty) = A^{-1} Y(\infty) A^{-T} + BB^T$$

If we set

$$(\bar{A}^{-1}) = \left[\begin{array}{c|c} A_1 & \mathbf{0} \\ \hline \mathbf{0} & A_2 \end{array}\right] = \left[\begin{array}{c|cc} A_u^{-1} & 0 & 0 \\ \hline 0 & A_s^{-1} & 0 \\ 0 & 0 & A_c^{-1} \end{array}\right], \quad \bar{B} = \left[\begin{array}{c} B_1 \\ B_2 \end{array}\right] = \left[\begin{array}{c} B_u \\ \hline B_s \\ B_c \end{array}\right],$$

$$Y(k) = \left[\begin{array}{c|c} Y_{11} & Y_{12} \\ \hline Y_{21} & Y_{22} \end{array}\right]$$

where A_u, A_s and A_c have the characteristic exponents with positive, negative and zero real parts respectively. Note that the order of submatrices are different from Eq. (19). Since $Y(k) = \sum_{j=0}^{k-1} A^j BB^T (A^T)^j \geq 0$ is symmetric, $Y_{12} = Y_{21}$. Then Eq. (16) becomes

$$Y_{11}(k+1) = A_1 Y_{11}(k) A_1^T + B_1 B_1^T, \;\; Y_{11}(0) = \mathbf{0} \tag{74}$$

$$Y_{12}(k+1) = A_1 Y_{12}(k) A_2^T + B_1 B_2^T, \;\; Y_{12}(0) = \mathbf{0} \tag{75}$$

$$Y_{22}(k+1) = A_2 Y_{22}(k) A_2^T + B_2 B_2^T, \;\; Y_{22}(0) = \mathbf{0} \tag{76}$$

Inverse of $Y(k)$ is given by

$$Y^{-1}(k) = \begin{bmatrix} Y_{11}^{-1} + Y_{11}^{-1} Y_{12} S^{-1} Y_{21} Y_{11}^{-1} & -Y_{11}^{-1} Y_{12} S^{-1} \\ -S^{-1} Y_{21} Y_{11}^{-1} & S^{-1} \end{bmatrix}$$

$$S \triangleq Y_{22} - Y_{21} Y_{11}^{-1} Y_{12}$$

After some matrix manipulation, we can obtain

$$S(k+1) = A_2 S(k) A_2^T + (B_2 - A_2 Y_{21}(k) Y_{11}^{-1}(k) A_1^{-1} B_1) X (B_2 - A_2 Y_{12}(k) Y_{11}^{-1}(k) A_1^{-1} B_1)^T$$

$$X \triangleq (I + B_1^T A_1^{-T} Y_{11}^{-1}(k) A_1^{-1} B_1)^{-1} > 0$$

Since $\lambda(A_2) \geq 1$, $S(k) > 0$ is monotone increasing and this implies $S(k)^{-1} > 0$ is monotone decreasing. Therefore $S(k) \to 0$ as $k \to \infty$. It also follows that $Y_{12}, Y_{21} \to 0$. Finally, $Y(k)^{-1}$ as $k \to \infty$ becomes

$$\lim_{k\to\infty} Y^{-1}(k) = \begin{bmatrix} Y_{11}^{-1} & 0 \\ 0 & 0 \end{bmatrix} \tag{77}$$

where Y_{11} is solution to the Lyapunov equation:

$$A_1^{-1} Y_{11} A_1^{-T} + \left(\int_0^T \phi_{11}^T(\tau, t_0) B_1 B_1^T \phi_{11}(\tau, t_0) d\tau \right) = 0 \tag{78}$$

where A_1 has unstable the characteristic exponents of e^{MT} and ϕ_{11} is the state transition matrix of unstable subsystem. The rest of the lemma can be proved similarly to the proof of Lemma 3.1.

References

[1] Howell, K., Barden, B. T., and Lo, M. W., "Application of Dynamical Systems Theory to Trajectory Design for a Libration Point Mission," *Journal of the Astronautical Sciences*, Vol. 45, No. 2, 1997, pp. 161–178.

[2] Gómez, G., Llibre, J., Martınez, R., and Simó, C., *Dynamics and Mission Design Near Libration Point Orbits–Volume 1: Fundamentals: The Case of Collinear Libration Points*. World Scientific, London, 2001.

[3] Gómez, G., Koon, W., Lo, M. W., Marsden, J. E., Masdemont, J., and Ross, S. D., "Invariant manifolds, the Spatial Three-Body Problem and Space Mission Design," *Advances in the Astronautical Sciences*, Vol. 109, pp. 3–22.

[4] Koon, W. S., Lo, M. W., Marsden, J. E., and Ross, S. D., "The Genesis Trajectory and Heteroclinic Cycles," *Proceedings of the AAS/AIAA Astrodynamics Specialist Conference*, 1999.

[5] Folta, D. C., Pavlak, T. A., Haapala, A. F., Howell, K. C., and Woodard, M. A., "Earth–Moon libration point orbit stationkeeping: theory, modeling, and operations," *Acta Astronautica*, Vol. 94, No. 1, 2014, pp. 421–433.

[6] Pierson, B. L. and Kluever, C. A., "Three-Stage Approach to Optimal Low-Thrust Earth-Moon Trajectories," *Journal of Guidance, Control, and Dynamics*, Vol. 17, No. 6, 1994, pp. 1275–1282.

[7] Kluever, B. L.C. A .and Pierson, "Optimal Low-Thrust Three-Dimensional Earth-Moon Trajectories," *Journal of Guidance, Control, and Dynamics*, Vol. 18, No. 4, 1995, pp. 830–837.

[8] Mingotti, G., Topputo, F., and Bernelli-Zazzera, F., "Low-Energy, Low-Thrust Transfers to the Moon," *Celestial Mechanics and Dynamical Astronomy*, Vol. 105, No. 1-3, 2009, pp. 61–74.

[9] Mingotti, G. and Gurfil, P., "Mixed Low-Thrust Invariant-Manifold Transfers to Distant Prograde Orbits around Mars," *Journal of Guidance, Control, and Dynamics*, Vol. 33, No. 6, 2010, pp. 1753–1764.

[10] Mingotti, G., Topputo, F., and Bernelli-Zazzera, F., "Earth–Mars Transfers with Ballistic Escape and Low-Thrust Capture," *Celestial Mechanics and Dynamical Astronomy*, Vol. 110, No. 2, 2011, pp. 169–188.

[11] Pergola, P., Geurts, K., Casaregola, C., and Andrenucci, M., "Earth–Mars Halo to Halo Low Thrust Manifold Transfers," *Celestial Mechanics and Dynamical Astronomy*, Vol. 105, No. 1-3, 2009, pp. 19–32.

[12] Dellnitz, M., Junge, O., Post, M., and Thiere, B., "On Target for Venus–Set Oriented Computation of Energy Efficient Low Thrust Trajectories," *Celestial Mechanics and Dynamical Astronomy*, Vol. 95, No. 1-4, 2006, pp. 357–370.

[13] Mingotti, G., Sánchez, J., and McInnes, C., "Combined low-thrust propulsion and invariant manifold trajectories to capture NEOs in the Sun–Earth circular restricted three-body problem," *Celestial Mechanics and Dynamical Astronomy*, Vol. 120, No. 3, 2014, pp. 309–336.

[14] Senent, J., Ocampo, C., and Capella, A., "Low-thrust variable-specific-impulse transfers and guidance to unstable periodic orbits," *Journal of Guidance, Control, and Dynamics*, Vol. 28, No. 2, 2005, pp. 280–290.

[15] Ozimek, M. and Howell, K. C., "Low-Thrust Transfers in the Earth-Moon System, Including Applications to Libration Point Orbits," *Journal of Guidance, Control, and Dynamics*, Vol. 33, No. 2, 2010, pp. 533–549.

[16] Longuski, J. M., Guzmán, J. J., and Prussing, J. E., *Optimal Control with Aerospace Applications*. Springer, 2014.

[17] Shibata, M. and Ichikawa, A., "Orbital Rendezvous and Flyaround based on Null Controllability with Vanishing Energy," *Journal of Guidance, Control, and Dynamics*, Vol. 30, No. 4, 2007, pp. 934–945.

[18] Anderson, R. L. and Lo, M. W., "Role of invariant manifolds in low-thrust trajectory design," *Journal of Guidance, Control, and Dynamics*, Vol. 32, No. 6, 2009, pp. 1921–1930.

[19] Mingotti, G., Topputo, F., and Bernelli-Zazzera, F., "Optimal Low-Thrust Invariant Manifold Trajectories via Attainable Sets," *Journal of Guidance, Control, and Dynamics*, Vol. 34, No. 6, 2011, pp. 1644–1656.

[20] Fairman, F. W., *Linear Control Theory: the State Space Approach*. John Wiley & Sons, 1998, Chap. 2, pp.186–189.

[21] Bryson, A. E. and Ho, Y. C., *Applied Optimal Control: Optimization, Estimation, and Control*. Taylor & Francis, New York, 1975, Chap. 5.

[22] Lawden, D. F., *Analytical Methods of Optimization*. Dover, Mineola, NY, 2006, Chap. 3.

[23] Perko, L., *Differential Equations and Dynamical Systems*, Vol. 7. 2001, pp. 220–223.

[24] Scheeres, D. J., "Navigation of Spacecraft in Unstable Orbital Environments," *International Conference on Libration Point Orbits and the Applications*, World Scientific, 2003, pp. 399–438.

[25] Szebehely, V., *Theories of Orbits: The Restricted Problem of Three Bodies*. 1967, pp.602–629.

[26] Scheeres, D. J., *Orbital Motion in Strongly Perturbed Environments*. 2012, pp. 306–307, 312–316.